Solar Energy Materials & Solar Cells 92 (2008) 1327–1335

Contents lists available at ScienceDirect

Solar Energy Materials & Solar Cells

journal homepage: www.elsevier.com/locate/solmat

All solution processed tandem polymer solar cells based on thermocleavable materials ☆

Ole Hagemann [a], Morten Bjerring [b], Niels Chr. Nielsen [b], Frederik C. Krebs [a,*]

[a] Risø National Laboratory for Sustainable Energy, Polymer Department, Technical University of Denmark, Frederiksborgvej 399, DK-4000 Roskilde, Denmark
[b] Center for Insoluble Protein Structures, Interdisciplinary Nanoscience Center (iNANO) and Department of Chemistry, University of Aarhus, DK-8000 Aarhus C, Denmark

ARTICLE INFO

Article history:
Received 28 February 2008
Received in revised form
28 April 2008
Accepted 8 May 2008
Available online 24 June 2008

Keywords:
Tandem cells
Fullerene free
Vacuum free
Polymer solar cells
P3MHOCT
P3TMDCTTP
P3CT
P3CTTP
PT
PTTP
Zinc oxide
Air stability
Air processing

ABSTRACT

Multilayer tandem polymer solar cells were prepared by solution processing using thermocleavable polymer materials that allow for conversion to an insoluble state through a short thermal treatment. The problems associated with solubility during application of subsequent layers in the stack were efficiently solved. Devices comprised a transparent front cathode based on solution processed zinc oxide nanoparticles, a large band gap active layer based on a bulk heterojunction between zinc oxide and poly(3-carboxydithiophene) (P3CT) followed by a layer of PEDOT:PSS processed from water. The second cell in the stack employed a zinc oxide front cathode processed on top of the PEDOT:PSS layer from an organic solvent, a low band gap active layer based on a bulk heterojunction between zinc oxide and the novel poly(carboxyterthiophene-*co*-diphenylthienopyrazine) (P3CTTP) followed by a layer of PEDOT:PSS again processed from water and finally a printed silver electrode. The devices were prepared without the use of fullerenes and vacuum steps and employ only thermal treatments and orthogonal solvents. The devices exhibited operational stability in air without any form of encapsulation.

1. Introduction

1.1. The need for low band gap and tandem cells

Polymer solar cells [1–4] potentially offer roll-to-roll fabrication based entirely on solution processes with no involved vacuum steps. The most efficient devices reported to date however only achieve the high performance through a delicate interplay between processing technique, conditions and solvent [5,6], and currently the power conversion efficiency of single bulk heterojunction cells is limited to around 5% while higher power conversion efficiencies are possible from a theoretical point of view [7–9]. One approach to improve the power conversion efficiency is to employ low band gap materials [3] that efficiently harvest more of the available photons. While research in low band gap materials is actively ongoing, this has so far not resulted in power conversion efficiencies significantly above 5%. Another approach that has been employed with success is the concept of a tandem cell where two or more single junctions are stacked or juxtaposed (Fig. 1) in such a manner that light at both short and long wavelengths is efficiently harvested and converted [10–19]. The mode of preparation of the active layer falls in three categories: all vacuum processing, a combination of vacuum and solution processing and all solution processing. The first reports relied on stacked cells and due to the difficulty of depositing sequential layers by solution processing the realization of the concept was most easily achieved by means of vacuum deposition of small molecules [10–13]. Since a first layer can be solution processed and the second layer vacuum deposited this approach conceptually followed suite [14] along with all solution processed devices employing orthogonal solvents and carefully chosen interfacial layers [15–17]. This approach has led to the highest reported efficiency of 6.5% for a polymer solar cell [17].

The tandem solar cell has been treated from a theoretical point of view [18] and recently a novel concept was developed whereby the tandem solar cell is realized in a reflective geometry thus avoiding complex multilayer solution processing [19]. One of the

☆ A patent application covering this invention has been filed.

* Corresponding author. Tel.: +45 46 77 47 99.
E-mail address: frederik.krebs@risoe.dk (F.C. Krebs).

0927-0248/$ - see front matter © 2008 Elsevier B.V. All rights reserved.
doi:10.1016/j.solmat.2008.05.005

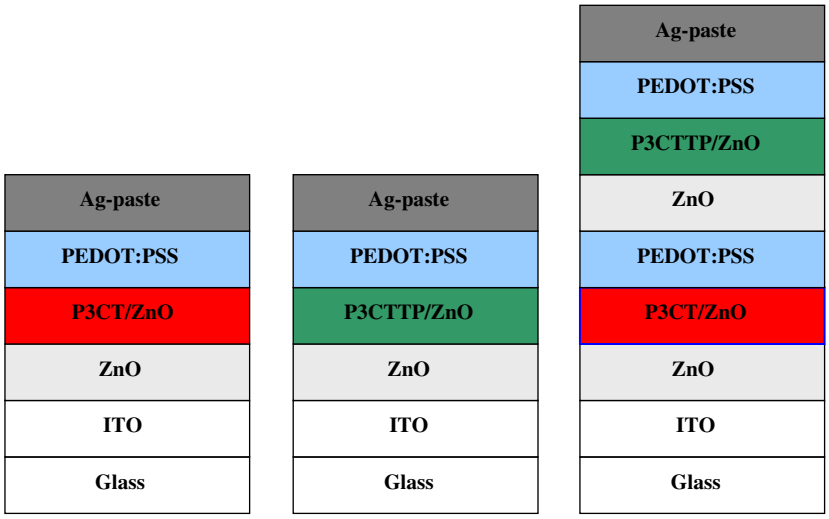

Fig. 1. Schematic representation of the single junction cells and the tandem cells prepared in this work employing wide band gap (P3CT) and a low band gap (P3CTTP) thermocleavable polymer materials.

strengths of polymer and organic solar cells is the possibility for all solution processing and while this has been demonstrated for tandem cells with evaporated metal electrodes there are still severe limitations to the choice of solvents and the order of application of the individual layers. The approach has so far employed different solvents for the different layers that are orthogonal in the sense that the next solvent in the process is a poor one for the material in the previously deposited layer.

1.2. The need for thermocleavable materials

Advanced processing techniques depend on the properties of the materials employed and in order to have a large degree of processing freedom it is necessary to put extra functionality into the materials. Generally, it cannot be anticipated that known materials can be processed using new techniques and most often modifications to the materials properties must be made. One challenge is, for instance, the solution processing of multilayer films of conjugated materials. The problem here is that once the first layer is formed and a dry film is obtained, the processing of the next layer from solution is difficult due to the solvent employed, which may either totally (or partially) dissolve the first layer unless one explores the choice of solvent. In the extreme case one layer may be processed from water and the following layer from, for instance, an organic solvent that does not dissolve the first layer. It is a possible scheme but requires that the solubility properties of the various layers are controlled according to the solvents employed. It is however not practical to have that constraint when many layers have to be processed on top of each other. In the case of tandem cells employing two stacked devices you need at least 6 layers and probably more. In the case of the devices presented here a total of 7 layers were required that were processed from solution. From this point of view, it is desirable to be able to switch off the solubility once a layer has been formed.

The concept of thermocleavable materials fulfills this requirement. In thermocleavable materials one explores the lability of a bond in the molecule. The labile bond is chosen as the linker between the group that conveys solubility and the active material backbone. In this case the solubilizing group is a branched alkyl chain attached to the active conjugated polymer backbone through an ester bond. When heated this bond breaks, eliminating a volatile alkene and leaving the polymer component insoluble. Using this method there is no limit on the choice of solvent when processing the subsequent layers. A prototypical example is poly-(3-(2-methylhexan-2-yl)-oxycarbonyldithiophene (P3MHOCT) that is a conjugated polymer with a polythiophene backbone and ester groups substituted onto the backbone. When heated to around ~200 °C an alkene is eliminated and the insoluble and carboxylated poly(3-carboxydithiophene (P3CT) is obtained as outlined in Fig. 2. P3CT can upon heating to higher temperatures of around ~300 °C give native polythiophene through decarboxylation. This thermal processing of P3MHOCT was studied by solid-state NMR on ^{13}C labeled P3MHOCT [20,21]. It was thus of interest to prepare analogous materials with different optical properties that had the same thermocleavable properties. We chose to prepare the low band gap polymer P3TMDCTTP, which is a copolymer of a diphenylthienopyrazine and terthiophene, and to characterize it by solid-state NMR to firstly establish if the thermocleavage was generic and if one could access both the carboxylated form and the decarboxylated form through thermal processing at two different temperatures and secondly, to employ this material in multilayer and tandem solar cells.

In this manuscript, we present this new approach where the materials can be processed from solution and made insoluble by a thermal treatment such that subsequent layers can be deposited from any solvent including the possibility of using the same solvent throughout the process. We present the detailed characterization of these novel materials using solid-state NMR and also demonstrate the application in a tandem cell.

2. Experimental

2.1. General synthesis

The synthetic approach of the thermocleavable low band gap precursor polymer, P3TMDCTTP, is outlined in Fig. 3. All reagents and solvents were standard grade. Regiorandom P3MHOCT was prepared as described in the literature [22]. The polymer had the following properties: $M_n = 11{,}600\,g\,mol^{-1}$, $M_w = 28{,}200\,g\,mol^{-1}$, $M_p = 27{,}500\,g\,mol^{-1}$, PD = 2.6.

2.2. Synthesis of (2,5,9-trimethyldecan-2-yl)-2,5-dibromothiophene-3-carboxylate

2,5-Dibromothiophene-3-carboxylic acid (10.0 g, 35 mmol) and 2-chloro-3,5-dinitropyridine (7.8 g, 38.5 mmol 1.1 eq.) were dis-

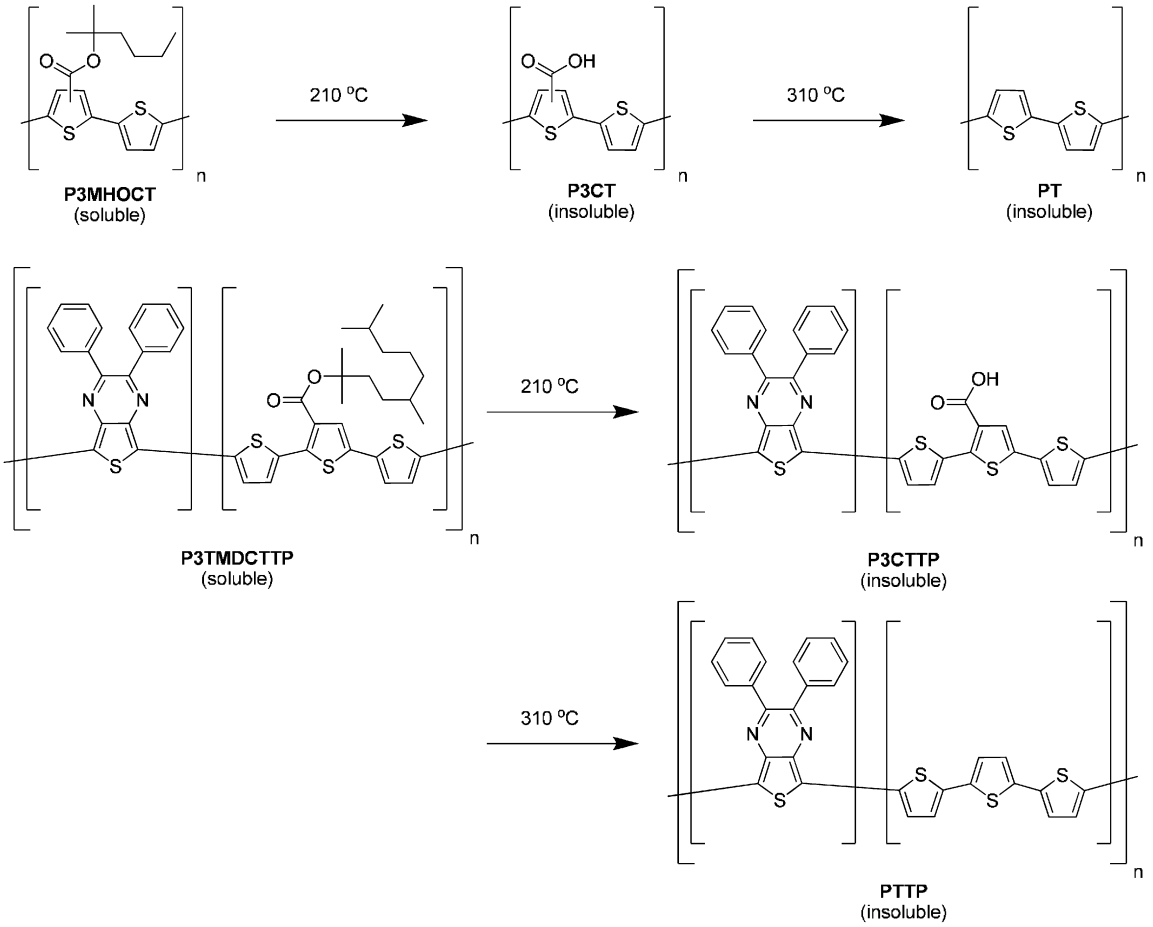

Fig. 2. Thermocleavage of the polymers P3MHOCT and P3TMDCTTP to P3CT and P3CTTP at 210 °C and further to PT and PTTP at 310 °C.

solved in dry pyridine under argon. The mixture was heated to approx. 40 °C for 30 min. 2,5,9-Trimethyl-decan-2-ol (7.7 g 38.5 mmol 1.1 eq) was added and the mixture is stirred at 120 °C over night. After cooling to ambient temperature, the mixture was poured into a mixture of water (300 mL), light petroleum (300 mL) and $NaHCO_3$(aq) (100 mL, 2 M). The aqueous phase was extracted with light petroleum (3×100 mL), and the combined organic phases were dried over $MgSO_4$ and evaporated to give a light yellow oil. The desired product was purified by flash chromatography using heptane as base solvent and extracted with 2% ethyl acetate to give a colorless oil. Yield: 5.1 g (34%). ^{1}H NMR ($CDCl_3$): δ: 0.88 (t, 9H, $J = 7$ Hz), 1.09–1.32 (m, 8H), 1.35–1.44 (m, 2H), 1.56 (s, 6H), 1.80–1.92 (m, 2H), 7.29 (s, 1H)). ^{13}C NMR ($CDCl_3$) δ: 19.7, 22.6, 22.7, 24.8, 26.1, 26.2, 28.0, 30.8, 33.0, 37.1, 38.2, 39.3, 85.0, 110.9, 118.0, 131.9, 133.4, 159.9.

2.3. Synthesis of 2,3-diphenyl-5,7-bis(5-(trimethylstannyl)thiophen-2-yl)thieno[3,4-b]pyrazine

A solution of LDA was prepared as follows: THF (10 mL) was cooled to −10 °C and *n*-BuLi (1.6 M, in hexane, 10 mL, 16 mmol) was added dropwise. The mixture was stirred for 10 min and diisopropylamine (2.5 mL, 18 mmol) in THF (7.5 mL) was added dropwise. The mixture was stirred for 30 min at −10 °C. and used directly. LDA solution (20 mL, 11 mmol, 5 eq.) was added dropwise to a solution of 2,3-diphenyl-di-thiophen-2-yl-thieno(3,4-b)pyrazine (1.0 g, 2.2 mmol) in THF (50 mL) at −78 °C. A color change from green to dark purple was observed. After 1 h at −78 °C (2.6 g, 13 mmol) of trimethylstannyl chloride dissolved in dry THF (7 mL) was added over a period of 5 min. After the mixture had reached ambient temperature it was evaporated to dryness and recrystallized from heptane, to give a purple solid. Yield: 1.1 g (64%). ^{1}H NMR ($CDCl_3$): δ: 0.44 (s, 18H), 7.22 (d, 2H, $J = 4$ Hz), 7.33–7.40 (m, 6H), 7.62 (dd, 4H, $J1 = 8$ Hz, $J2 = 1$Hz), 7.87 (d, 2H, $J = 4$ Hz). ^{13}C NMR ($CDCl_3$) δ: −8.2, 124.9, 126.1, 128.0, 128.9, 130.0, 135.6, 137.5, 139.2, 139.7, 140.2, 152.7.

2.4. Synthesis of regiorandom poly-[(3′-(2,5,9-trimethyldecan-2-yl)-oxy-carbonyl)-[2,2′;5′,2″]terthiophene-1,5″-diyl)-co-(2,3-diphenylthieno[3,4-b]pyrazine-5,7-diyl)] (P3TMDCTTP)

Compound (2) (300 mg, 0.3854 mmol) and compound (1) (180.5 mg, 0.3854 mmol) were dissolved in dry toluene under argon, Pd_2dba_3 (12.5 mg,) and tri-*o*-tolylphosphine (65 mg) was added. *N*-methyldicyclohexyl amine (0.5 mL) was added after 5 min. The mixture was refluxed for 20 h. The mixture was concentrated to half the original volume on a rotary evaporator in vacuum and the residue was poured into 8 volumes of methanol. The precipitate was isolated by filtration, washed with methanol and dried to give a dark green powder. Yield: 198 mg (67%). ^{1}H NMR ($CDCl_3$): δ: 0–79–0.86 (m, 9H), 1.05–1.35 (m, 10H), 1.50–1.60 (m, 6H), 1.74–1.90 (m, 2H), 7.30–7.50 (m, 9H), 1.51–1.73 (m, 6H). SEC: $M_n = 37{,}300$, $M_w = 61{,}900$, $M_p = 49{,}300$, PD = 1.7.

2.5. Solid-state NMR experiments

The low band gap precursor polymer P3TMDCTTP was loaded into zirconia rotors (7.8 mg) and ^{1}H and ^{13}C MAS NMR spectra

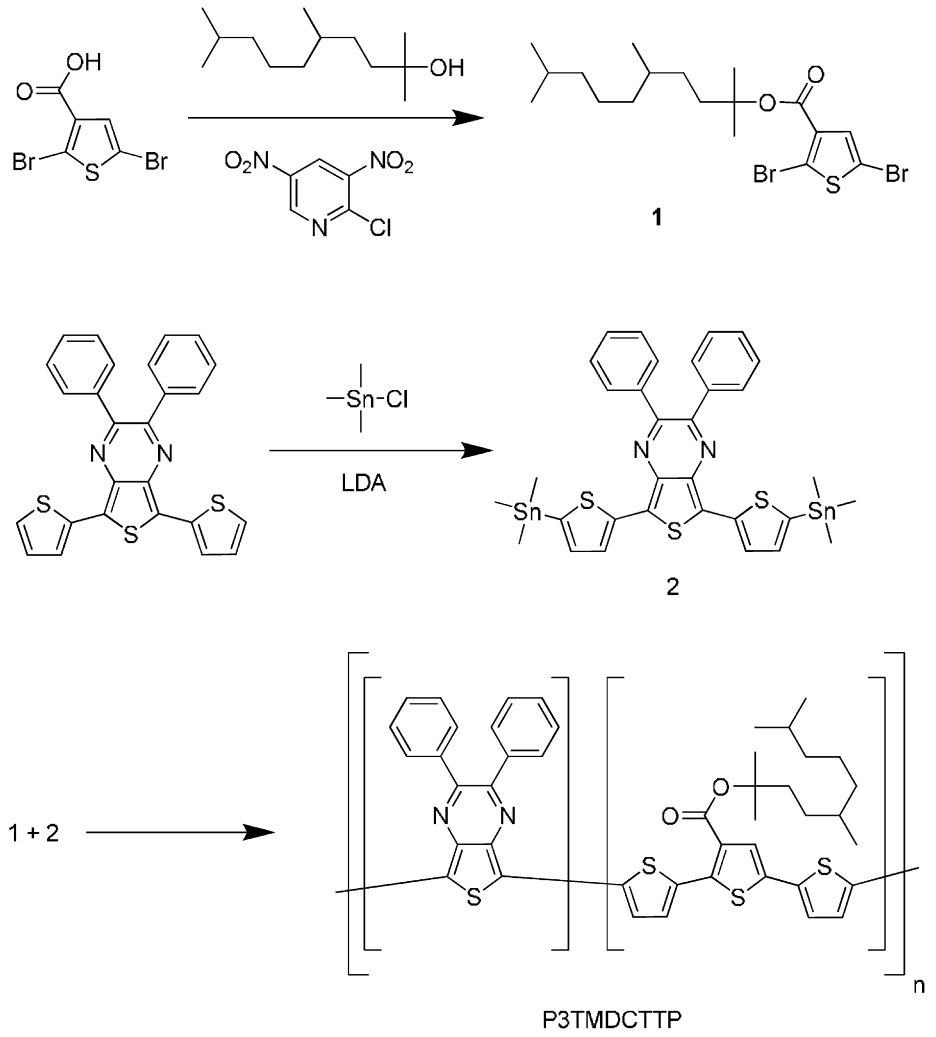

Fig. 3. Synthetic procedure to the thermocleavable low band gap polymer P3TMDCTTP.

were recorded. The thermal conversion of P3TMDCTTP to respectively P3CTTP and PTTP was subsequently performed by removal of the end caps and heating the zirconia rotor to a temperature of 210 °C (in the case of P3CTTP) and 310 °C (in the case of PTTP) in a high vacuum chamber at a pressure $<1\times10^{-6}$ mbar. The samples were kept at the desired temperatures for 30 min and then cooled down before removal from the chamber. The end caps were replaced and the NMR spectra were recorded. All NMR experiments were recorded on a 400 MHz (^{1}H frequency) Bruker Avance spectrometer using a 2.5 mm triple-resonance Bruker probe and operating at room temperature. For the ^{13}C spectra, cross polarization (CP) was used to improve sensitivity and a magic-angle spinning (MAS) speed of 10 kHz was applied. A total of 2048 subsequent scans were added for each ^{13}C spectrum. 2D ^{1}H single-quantum versus double-quantum correlation spectra were recorded using the BABA (back to back) pulse sequence [23] with an applied spinning speed of 30 kHz. For these experiments, 16 scans were added for each t^1 increment.

2.6. Preparation of zinc oxide nanoparticle solutions and polymer solutions

A procedure leading to soluble zinc oxide nanoparticles and their application to solar cells was first disclosed by Wormelsdorf et al. [24–26] in a series of patents. Later on Beek et al. [27] used these particles in polymer solar cells. A modified version of this method was employed for mixtures with P3MHOCT [28] and this method was also employed in this work. Solutions of P3MHOCT and P3TMDCTTP were prepared in chlorobenzene and mixed with a zinc oxide nanoparticle solution to reach a final concentration of 25 mg mL^{-1} of the polymer and 50 mg mL^{-1} of zinc oxide nanoparticles.

2.7. Preparation of device films

The formation of the zinc oxide films, the polymer–zinc oxide nanoparticle films and the thermocleavage was carried out in a glovebox. The PEDOT:PSS films were applied in ambient air. For the tandem cells this implied removing the substrates from the glovebox environment after the first junction had been prepared followed by reintroduction into the glovebox after the PEDOT:PSS electrode had been applied and dried. The second junction was then prepared in the glovebox. Freshly cleaned glass-ITO substrates, where part of the ITO had been removed by etching, were used and firstly a layer of zinc oxide nanoparticles was spin coated at 800 rpm from a chlorobenzene solution (50 mg mL^{-1}). The dried nanoparticle film was annealed for 2 min on the hotplate at 210 °C. The substrate was then cooled and the active layer was spin coated at 800 rpm from chlorobenzene with P3MHOCT (25 mg mL^{-1}) or P3TMDCTTP (25 mg mL^{-1}) and the zinc oxide nanoparticles (50 mg mL^{-1}). After the film had dried it was heated on the hot plate at 210 °C for 2 min whereby P3MHOCT is

converted to P3CT and P3TMDCTTP is converted to P3CTTP. The conversion is in the case of P3MHOCT associated with a clearly visible color change from burgundy red to a bright red color. In the case of P3TMDCTTP the conversion is not as clearly visible to the eye but a distinct change in color from a clear green to a more pale tone is visible. The completeness of the thermocleavage was tested by rubbing a cotton bud wetted in chlorobenzene across an area of the film that was not going to be part of the active area. The cleaved films were completely insoluble. The substrates with the composite films were removed from the glovebox and a layer of PEDOT:PSS was applied by firstly layering the PEDOT:PSS solution over the substrate and then spinning the substrate at 2800 rpm. The films were then dried at 120 °C for 10 min in air and either used to make a single junction device or reintroduced into the glovebox in order to make tandem devices.

2.8. Application of back electrodes

The silver back electrode was based on Dupont 5007 and is a silver migration resistant polymer thick film conductor that can be cured at 130–140 °C for 3 min. The silver electrode was applied by doctor blading through a mask giving two devices on each substrate with a quadratic active area measuring 1 cm^2. The devices were tested when freshly made but as observed earlier, they improved upon standing in the dark for 24 h [28] and characterization was generally carried out after 24 h in the dark under atmospheric conditions (25°C, ~20% oxygen, 35 ± 5% relative humidity).

2.9. Device testing and lifetime measurements

The devices were illuminated using a solar simulator from Steuernagel lichttechnik, KHS 575 by placing the unencapsulated device under the sun simulator in the ambient atmosphere with a relative humidity of 35 ± 5%. The temperature of the devices during the measurements was typically 72 ± 2 °C. The luminous intensity and emission spectrum of the solar simulator approaches AM1.5G and was set to 1000 W m^{-2} using a bolometric radiometer from Eppley Laboratories. The incident light intensity was monitored continuously every 60 s during the measurements using a high-temperature bolometric radiometer from Kipp and Zonen. No corrections were made for mismatch. *IV*-curves were recorded with a Keithley 2400 Sourcemeter from −1 to +1 V in steps of 10 mV with a speed of 0.1 s $step^{-1}$. IPCE measurements were recorded using a high-power spectrometer comprising a water cooled Xenon lamp, a blazed diffraction grating as described in the literature [29] that had been improved with a longer source to grating distance and cylindrical lenses to improve light intensity and bandwidth at the sample to 10 nm.

3. Results and discussion

3.1. Solid-state NMR of P3TMDCTTP

The ^{13}C CP MAS spectrum of P3TMDCTTP is shown in Fig. 4a. The spectrum is dominated by signals from the aliphatic carbons at 10–50 ppm and the aromatic carbons at 120–158 ppm. In addition, the signal from the quaternary carbon is seen at 84 ppm, and the carbonyl gives rise to the signal at 162 ppm. After the first thermocleavage at 210 °C, the ^{13}C spectrum in Fig. 4b was recorded. This spectrum confirms the elimination of the aliphatic sidechain, as the signals in the aliphatic region are highly reduced. Furthermore, the major part of the, although rather weak, carbonyl signal is shifted to 170 ppm, indicating a change in functionality from an ester group to a carboxylic acid. The same chemical shift change was also seen in the P3MHOCT→P3CT thermocleavage [20,21]. The second thermocleavaged product obtained from the heating to 310 °C gives the ^{13}C spectrum shown in Fig. 4c. It is seen that the carbonyl signals vanish as predicted from Fig. 2, and besides a small amount of aliphatic contaminant, only aromatic carbons are left. We therefore conclude that decarboxylation was achieved in accordance with Fig. 2. In order to highlight the chemical shift change and the disappearing of

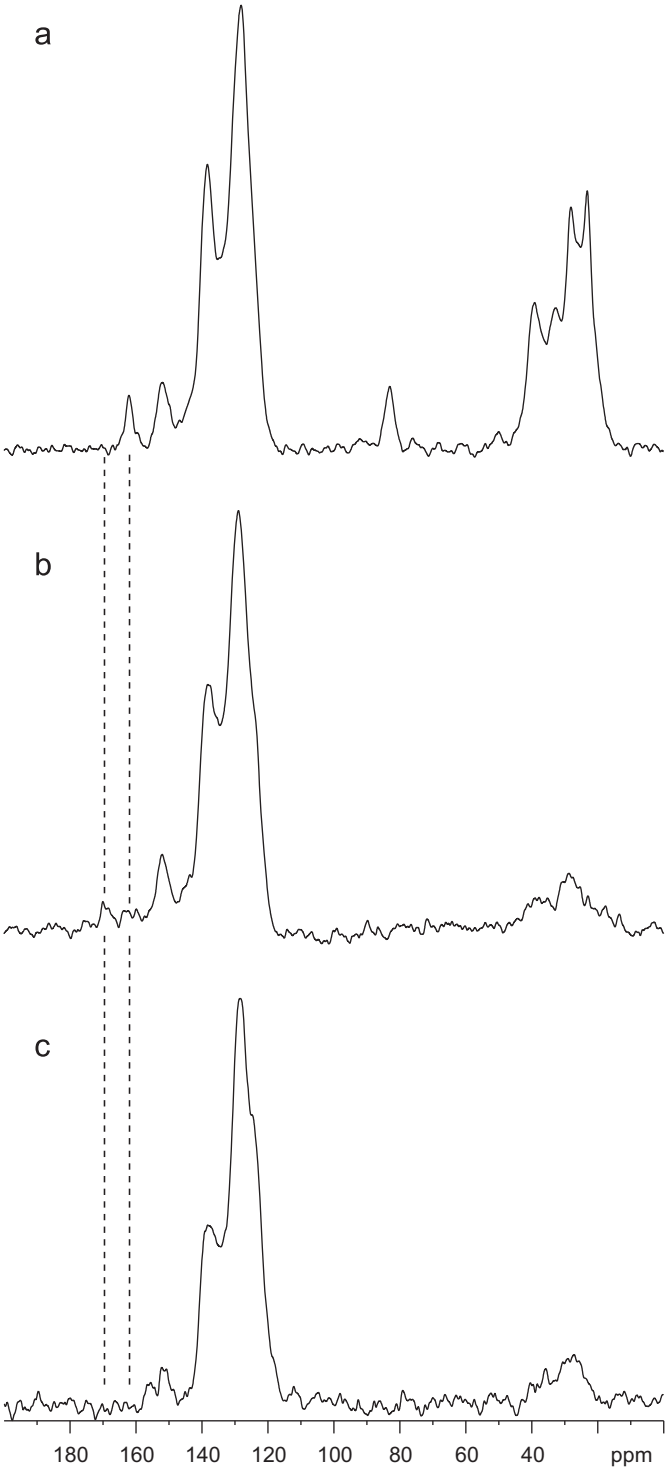

Fig. 4. 1D ^{13}C CP MAS spectra of P3TMDCTTP (a), P3CTTP (b), and PTTP (c). The dashed lines at 162 and 170 ppm are drawn as a guide for the eyes.

signals in the carbonyl region, dashed lines are drawn at the carboxylic ester position (162 ppm) and carboxylic acid position (170 ppm). 1D ^{1}H experiments were also carried out on P3TMDCTTP and the two thermocleavaged products and these spectra (not shown) support the conclusions from the ^{13}C experiments.

With the confirmation of the P3CTTP polymer as the first thermocleavaged product, it was of great interest to investigate this polymer network in more detail. For this purpose, two-dimensional (2D) double quantum (DQ) ^{1}H NMR spectroscopy at fast MAS is well suited. In a 2D DQ spectrum, resonances in the indirect dimension appear at the sum of the involved frequencies. DQ coherences (and thereby resonances in the spectra) involve two different spins, and are produced via the ^{1}H–^{1}H dipolar couplings, depending directly on the internuclear distances.

In practice, this means that observation of a peak in a 2D DQ spectrum is indicative of a proton–proton distance of at most 3 Å [30]. The 2D DQ spectrum of P3CTTP (not shown) is dominated by a very strong and broad signal centered at (6.7, 13.4 ppm), indicating aromatic protons in close proximity, as expected. Three 1D traces from the 2D spectrum were taken parallel to the indirect dimension at 0.75 ppm (aliphatic protons), 6.7 ppm (aromatic protons), and 13.3 ppm (acid protons), where the chemical shift values represent aliphatic protons, aromatic protons, and carboxylic acid protons respectively. The slices with varying amplification given as fractions of the intensity of the dominating peak were examined (see Appendix A). A large peak in the slice through 6.7 ppm was observed which represents the aromatic-aromatic 'autopeak' mentioned above. The most interesting slice is through 13.3 ppm which shows a weak, however certainly above the noise, peak centered around 27 ppm. This peak indicate that two carbonyl protons are in close proximity, and since the proton-proton distances for carbonyls on the same polymer strand exceed 3 Å, we conclude that carboxylic acid groups create a hydrogen bonding network between the polymer chains. There was also a peak at ca. 20 ppm in the slice through 13.3 ppm showing that the carbonyl protons are also close to aromatic carbons, which is expected. For the aliphatic region in the slice through 0.75 ppm, peaks around 1.5 and 7.5 ppm are consequences of aliphatic protons close to each other and aliphatic protons close to aromatic protons, respectively.

3.2. Preparation of tandem solar cells

The preparation of multilayer solar cells using thermocleavable materials was straightforward and efficiently solves all the problems associated with unintentional solubilization of underlying layers during processing of subsequent layers. In Fig. 5, the absorptions of the device films are shown. It is clear that both P3CT and P3CTTP absorb in the 400–600 nm region whereas P3CTTP absorb in the range 600–900 nm.

The absorption spectrum of the tandem film is essentially the sum of the absorption spectra for P3CT and P3CTTP. There is however a higher absorption in the tandem film due to the additional PEDOT:PSS layer that absorbs in the region of 800–1100 nm and probably also some scattering loss from the multilayer structure. The preparation of the devices was fast and in the case of all solution processed tandem devices the entire preparation could be completed in less than 1 h including removal from the glovebox after the first cell had been made in order to add the PEDOT:PSS layer. In the case of the experiments involving a gold recombination layer between the first and second cells, longer preparation times were required due to pumping to a suitable vacuum for the evaporation of gold.

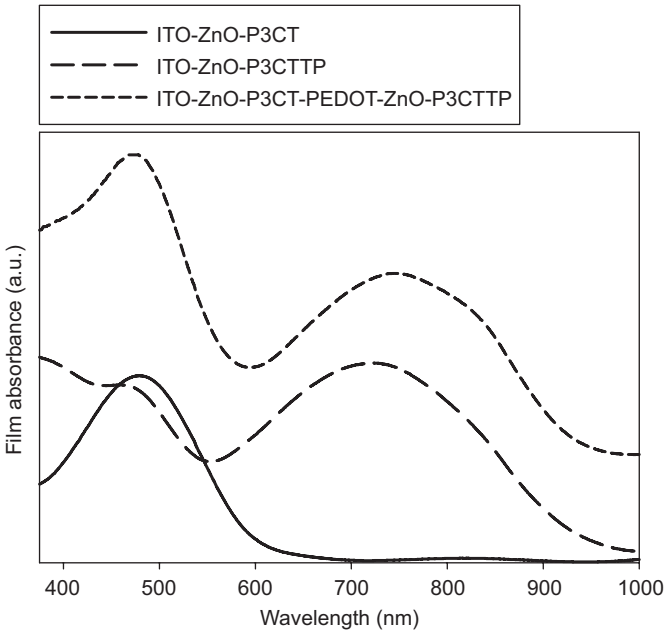

Fig. 5. UV–vis of the device films as prepared on glass-ITO substrates. The active layer was a bulk heterojunction of the polymer and zinc oxide nanoparticles. The high absorption in the tandem cell at wavelengths above 900 nm is due to the PEDOT:PSS layer between the two stacks and possibly some scattering loss in the multilayer structure.

3.3. Performance of single junctions and tandem device

In the tandem cell a wide band gap device is placed in front of a low band gap device and ideally the open-circuit voltage of the tandem device equals the sum of the open-circuit voltage for the two devices taken individually. In practical terms, the open-circuit voltage of the tandem device may be somewhat lower due to voltage drops at the various interfaces in the multilayer device. As the two devices in the stack essentially are serially connected, the short-circuit current of the tandem device is determined by the device that gives the lowest current. This implies that the devices must be balanced in terms of short-circuit current to achieve the highest performance. Since the serial connection is in the middle of the device and is hidden from the experimenter it is problematic to access just one of the cells in the stack. The *IV*-curves for single and tandem devices based on P3CT and P3CTTP are shown in Fig. 6 and have been summarized in Table 1. In the case of single devices based on P3CT and P3CTTP the latter performs quite poorly in terms of short-circuit current and this also places a limit on the performance of the tandem cell as expected.

The short-circuit current of the tandem cells is about half the current observed for single devices based on P3CTTP and there must be some loss mechanism in the device which is also evident from the open-circuit voltage that ideally should be around 0.74 V whereas we observe only 0.54 V. The tandem cells prepared consistently presented higher voltages than the P3CT reference devices by about 50 mV and as such the principle works while there is some serial resistance in the device that gives rise to a drop in voltage and current. This is also supported by the fill factor that consistently gave lower values than the single devices.

One explanation for this could be the PEDOT:PSS-ZnO junction connecting the two devices in the tandem cell. To test this, a thin layer of gold (5 nm) was evaporated onto the PEDOT:PSS layer in the P3CT device when preparing the tandem cell (see Fig. 7). The low band gap cells based on P3CTTP was subsequently prepared by spin coating the ZnO cathode by the P3TMDCTTP layer

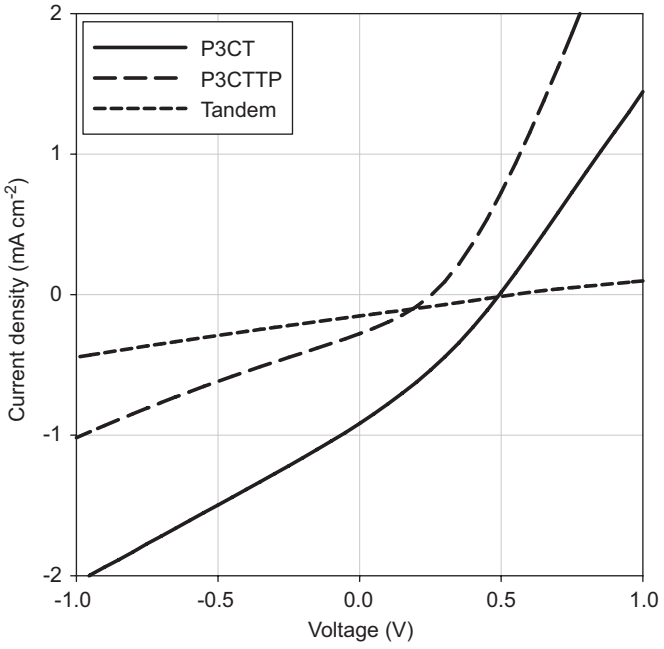

Fig. 6. *IV*-curves for the freshly prepared devices based on heterojunctions of P3CT/ZnO, P3CTTP/ZnO and a tandem cell of P3CT/ZnO in front of P3CTTP/ZnO (1000 W m^{-2}, AM1.5G, 72 ± 2 °C, ambient atmosphere, 30 ± 5% relative humidity).

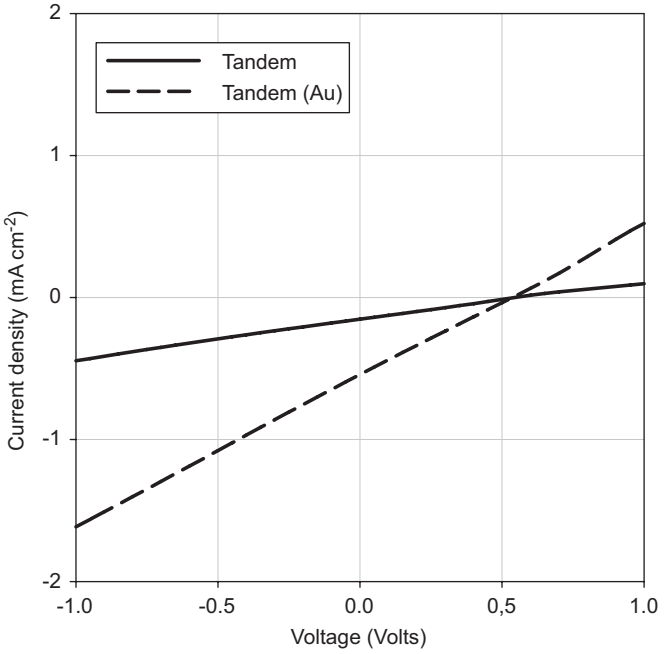

Fig. 7. A comparison of the performance of tandem cells with and without a thin gold recombination layer.

Table 1
Typical performance for the devices based on P3CT, P3CTTP and tandem cells

Device	I_{sc} (mA cm^{-2})	V_{oc} (V)	FF (%)	PCE (%)
P3CT	−0.91	0.49	29.6	0.13
P3CTTP	−0.28	0.25	31.1	0.02
Tandem	−0.15	0.54	25.8	0.02
Tandem (Au)	−0.54	0.54	24.6	0.07

followed by the thermal treatment, application of the final PEDOT:PSS layer and silver paste electrode. This lead to a dramatic increase in the short-circuit current but there was no increase in the voltage, which remained the same. The introduction of the gold recombination thus allows for the conclusion that the voltage drop is not at the PEDOT:PSS-ZnO interface while the addition of the recombination layer greatly affected the obtainable short-circuit current which by a large margin exceed the value generally obtained for single devices based on P3CTTP. While the gold layer would seem advantageous from a device performance point of view, there is the large drawback of a vacuum evaporation step. The strength of the approach employed for these devices is that they can be prepared by simple processing with no requirements for vacuum steps or fullerene derivatives. The current drawback is admittedly the low performance. An analysis of the IPCE spectra for the devices was performed (see Fig. 8). Firstly, to establish qualitatively whether the single devices performed in the expected wavelength regions, and secondly, to test the workings of the tandem cell. The single devices based in P3CT and P3CTTP behaved as expected with P3CT being the device demonstrating the highest values for the IPCE. The P3CTTP devices performed over a large range of wavelengths all the way up 900 nm in accordance with the absorption spectrum (see Fig. 5). For the tandem cell however there was, as expected, a lower response in the region from 400 to 600 nm where both P3CT and P3CTTP absorb light. At the longer wavelengths of 600–900 nm, however, the tandem cell showed no photocurrent in spite of the fact that the P3CTTP device is operational in this range. This is consistent

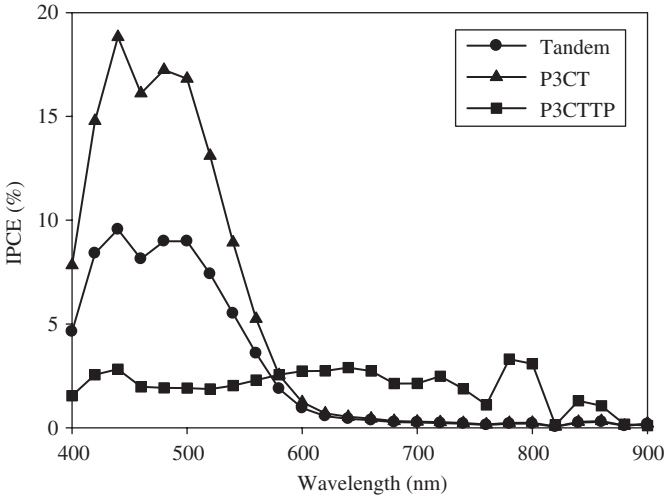

Fig. 8. IPCE data for single and tandem devices based on P3CT and P3CTTP. The peak in the IPCE data for single devices based in P3CTTP at around 780–800 nm are due to spectral lines in the light source that tend to overestimate the IPCE in that specific region.

with the observations reported by Kim et al. [17] where a light bias was employed to the cell that was not probed during IPCE measurements. In order for the tandem cell to produce a current both cells in the stack must be operational. In the 400–600 nm wavelength range this is the case and a significant IPCE is observed. In the 600–900 nm range only the P3CTTP device is operational and the P3CT device produces no current. The device is thus unable to show IPCE as observed. The magnitude of the IPCE values for these devices is not transferable to the performance under 1000 W m^{-2} and AM1.5G due to a strong non-linearity as described earlier [28]. Generally, devices based on P3CT more than double their performance when decreasing the illumination intensity from 1 sun (1000 W m^{-2}, AM1.5G) to typical indoor light intensities of 50–100 W m^{-2}.

3.4. Lifetime and stability of single and tandem junctions

Aside from the processing advantages conveyed by thermocleavable materials, they are believed to generally convey operational stability [31]. This has been demonstrated for P3CT during testing for more than 10,000 h under inert conditions [32,33], for encapsulated devices under outside conditions with the real sun as a light source [34] and finally in air stable devices [28]. The anticipation of operational stability for the thermocleavable material P3CTTP as described here was met. The devices prepared here were quite stable in air and followed the behavior described earlier for devices based on bulk heterojunctions of P3CT and ZnO nanoparticles [28].

The general observations for this type of device are: improvement of the performance upon leaving the devices in air in the dark after preparation, operational stability in air, recovery after being tested and left to repose in the dark (and air), and stability towards oxygen and humidity. The experiments performed here also confirm that the tandem cells exhibit the same stability as the individual materials. One interesting aspect was observed after significant periods of continuous testing (see Fig. 9) where the tandem nature of the tandem cell becomes more characteristic. In Fig. 9, the open-circuit voltages are plotted as a function of time. The sum of the single junction devices is also plotted and that equals the ideal open-circuit voltage for the tandem cell. After about 50 h of testing and onwards the open-circuit voltage of the tandem cells is significantly larger than the open-circuit voltage for the single junctions tested in parallel.

3.5. Perspectives and future work

A clearly identifiable advantage of thermocleavable materials is that they offer new levels of processing after the film has been formed. While it has been explored in this work for the purpose of switching the solubility of the active materials from soluble to insoluble one could easily envisage materials that contained alkyl groups or other solubilizing/organizing groups in addition to the thermocleavable groups. It would thus be possible to transform a material containing thermocleavable esters and alkyl groups into a material that contains only the alkyl groups. The advantages here could be processing stability and synthetic ease in cases where the acid containing materials are easier to obtain. In order to improve the performance of the devices demonstrated the junction between the two cells in the stack should be improved.

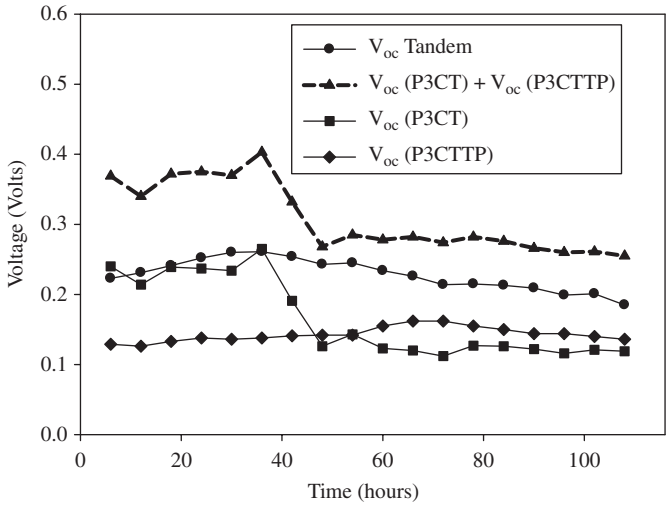

Fig. 9. Lifetime testing of a devices showing that the devices become more convincing tandem cells as the devices degrade.

This may involve the use of other oxides such as titanium, niobium or cerium. In terms of the performance of the materials themselves it is likely that the charge carrier properties are adversely affected by the thermal treatment and a better understanding on how to control these properties during thermal processing would be desired. It is clear that the elimination of the ester groups leads to a significant change in volume of the film and this will affect the ordering and packing of the molecules. The materials employed belong to the class of materials known as polythiophenes and copolymers of thiophene and thienopyrazine. Both material classes are well known and have been documented to exhibit good properties. From this point of view, most of the increase in performance should be sought in the method of thermal processing. It could however be an advantage to explore different substitution patterns for the ester groups. In the case of P3TMDCTTP-type polymers one could for instance attach the esters to the phenyl groups on diphenylthienopyrazine and explore whether there would be any advantages in doing so. Another route would be to explore other electron conductors. In this work zinc oxide nanoparticles were employed due to their low cost and easy routes to stable nanostructures. It should however be possible to prepare traditional fullerene derivatives with thermocleavable sidechains. In the context of fullerenes with thermal processing properties the advantages could be a stabilization of the morphology.

4. Conclusion

A low band gap polymer material (P3TMDCTTP) with thermocleavable properties was prepared and characterized. Solid state NMR experiments showed that the P3TMDCTTP material could be processed in exactly the same manner as P3MHOCT. Based on P3TMDCTTP one can gain access to the acid form P3CTTP and the decarboxylated form PTTP. Polymer solar cell devices based on bulk heterojunctions of P3CT, P3CTTP and zinc oxide nanoparticles were prepared and characterized. Furthermore, tandem polymer solar cells based on stacked P3CT and P3CTTP devices were demonstrated employing an inverted geometry that is free of fullerenes and evaporated back electrodes. The devices were prepared entirely by solution processing and no vacuum coating steps were employed. No encapsulation was employed and the devices could be stored in the dark under ambient conditions in air for extended periods of time without degradation. The performance of the tandem devices was inferior to simple devices based on P3CT due to the lower current obtained for P3CTTP devices. The poorer performance of the tandem solar cells as compared to the single P3CT devices is ascribed to a poor match between the individual cells. The open-circuit voltage for the tandem cells were shown to be higher than for the single junctions while the tandem devices present a significant voltage drop at one of the interfaces limiting the advantage of the more complex tandem cell in the current configuration. Devices based on P3CTTP and tandem cells were operationally stable in air thus adding evidence to the proposition that thermocleavable materials give rise to better operational stability.

Acknowledgments

This work was supported by the Danish Strategic Research Council (DSF 2104-05-0052 and 2104-07-0022), Danish National Research Foundation and the Danish Biotechnological Instrument Centre (DABIC). We would like to express sincere gratitude to Jan Alstrup for technical assistance.

Appendix A. Supplementary data

Supplementary data associated with this article can be found in the online version at doi:10.1016/j.solmat.2008.05.005.

References

[1] C.J. Brabec, N.S. Sariciftci, J.C. Hummelen, Plastic solar cells, Adv. Funct. Mater. 11 (2001) 15.
[2] H. Spanggaard, F.C. Krebs, A brief history of the development of organic and polymeric photovoltaics, Sol. Energy Mater. Sol. Cells 83 (2004) 125.
[3] E. Bundgaard, F.C. Krebs, Low band gap polymers for organic photovoltaics, Sol. Energy Mater. Sol. Cells 91 (2007) 954.
[4] S. Günes, H. Neugebauer, N.S. Sariciftci, Conjugated polymer-based organic solar cells, Chem. Rev. 107 (2007) 1324.
[5] G. Li, V. Shrotriya, J. Huang, Y. Yao, T. Moriarty, K. Emery, Y. Yang, High-efficiency solution processable polymer photovoltaic cells by self-organization of polymer blends, Nat. Mater. 4 (2005) 864.
[6] W. Ma, C. Yang, X. Gong, K. Lee, A.J. Heeger, Thermally stable, efficient polymer solar cells with nanoscale control of the interpenetrating network morphology, Adv. Funct. Mater. 15 (2005) 1617.
[7] S.R. Forrest, The limits to organic photovoltaic cell efficiency, MRS Bull. 30 (2005) 28.
[8] L.J.A. Koster, V.D. Mihailetchi, P.W.M. Blom, Ultimate efficiency of polymer/fullerene bulk heterojunction solar cells, Appl. Phys. Lett. 88 (2006) 093511, 1–3.
[9] M.C. Scharber, D. Mühlbacher, M. Koppe, P. Denk, C. Waldauf, A.J. Heeger, C.J. Brabec, Design rules for donors in bulk-heterojunction solar cells—towards 10% energy-conversion efficiency, Adv. Mater. 18 (2006) 789.
[10] A. Yakimov, S.R. Forrest, High photovoltage multiple-heterojunction organic solar cells incorporating interfacial metallic nanoclusters, Appl. Phys. Lett. 80 (2002) 1667.
[11] J. Xue, S. Uchida, B.P. Rand, S.R. Forrest, Asymmetric tandem organic photovoltaic cells with hybrid planar-mixed molecular heterojunctions, Appl. Phys. Lett. 85 (2004) 5757.
[12] J. Xue, S. Uchida, B.P. Rand, S.R. Forrest, 4.2% efficient organic photovoltaic cells with low series resistances, Appl. Phys. Lett. 84 (2004) 3013.
[13] D. Cheyns, H. Gommans, M. Odijk, J. Poortmans, P. Heremans, Stacked organic solar cells based on pentacene and C_{60}, Sol. Energy Mater. Sol. Cells 91 (2007) 399.
[14] A. Colsmann, J. Junge, C. Kayser, U. Lemmer, Organic tandem solar cells comprising polymer and small-molecule subcells, Appl. Phys. Lett. 89 (2006) 203506, 1–3.
[15] A. Hadipour, B. de Boer, J. Wilderman, F.B. Kooistra, J.C. Hummelen, M.G.R. Turbiez, M.M. Wienk, R.A.J. Janssen, P.W.M. Blom, Solution-processed organic tandem solar cells, Adv. Funct. Mater. 16 (2006) 1897.
[16] J. Gilot, M.M. Wienk, R.A.J. Janssen, Double and triple junction polymer solar cells processed from solution, Appl. Phys. Lett. 90 (2007) 143512, 1–3.
[17] J.Y. Kim, K. Lee, N.E. Coates, D. Moses, T.-Q. Nguyen, M. Dante, A.J. Heeger, Efficient tandem polymer solar cells fabricated by all-solution processing, Science 317 (2007) 222.
[18] N.K. Persson, O. Inganäs, Organic tandem solar cells—modelling and predictions, Solar Energy Mater. Solar Cells 90 (2006) 3491.
[19] K. Tvingstedt, V. Andersson, F. Zhang, Inganäs, Folded reflective tandem polymer solar cell doubles efficiency, Appl. Phys. Lett. 91 (2007) 123514, 1–3.
[20] M. Bjerring, J.S. Nielsen, N.C. Nielsen, F.C. Krebs, Polythiophene by solution processing, Macromolecules 40 (2007) 6012.
[21] M. Bjerring, J.S. Nielsen, A. Siu, N.C. Nielsen, F.C. Krebs, An explanation for the high stability of polycarboxythiophenes in photovoltaic devices—a solid-state NMR dipolar recoupling study, Sol. Energy Mater. 92 (2008) 772.
[22] J.S. Liu, E.N. Kadnikova, Y.X. Liu, M.D. McGehee, J.M.J. Fréchet, Polythiophene containing thermally removable solubilizing groups enhances the interface and the performance of polymer-titania hybrid solar cells, J. Am. Chem. Soc. 126 (2004) 9486.
[23] W. Sommer, J. Gottwald, D.E. Demco, H.W. Spiess, Dipolar heteronuclear multiple-quantum NMR spectroscopy in rotating solids, J. Magn. Reson. 113A (1995) 131.
[24] H. Womelsdorf, W. Hoheisel, G. Passing, Nanopartikuläres, redispergierbares fällungsoxid, German Patent (filing date 23.02.1999) DE 19907704 A1.
[25] H. Womelsdorf, W. Hoheisel, G. Passing, Process for producing nanoparticulate, redispersible zinc oxide gels, European Patent (filing date 11.02.2000) EP 1157064 B1.
[26] H. Womelsdorf, W. Hoheisel, G. Passing, Nanoparticulate, redispersible zinc oxide gels, Unites States Patent (patent date 23.03.2004) US 6,710,091 B1.
[27] W.J.E. Beek, M.M. Wienk, M. Kemerink, X. Yang, R.A.J. Janssen, Hybrid zinc oxide conjugated polymer bulk heterojunctions solar cells, J. Phys. Chem. B 109 (2005) 9505.
[28] F.C. Krebs, Air stable polymer photovoltaics based on a process free from vacuum steps and fullerenes, Sol. Energy Mater. Sol. Cells 92 (2008) 715.
[29] F.C. Krebs, M. Jørgensen, High power spectrometer for the characterization of photovoltaic cells in a controlled atmosphere or vacuum, Rev. Scientific Instrum. 74 (2004) 3438.
[30] I. Schnell, S.P. Brown, H.Y. Low, H. Ishida, H.W. Spiess, An investigation of hydrogen bonding in benzoxazine dimmers by fast magic-angle spinning and double-quantum ^{1}H NMR spectroscopy, J. Am. Chem. Soc. 120 (1998) 11784.
[31] M. Jørgensen, K. Norrman, F.C. Krebs, Stability/degradation of polymer solar cells, Sol. Energy Mater. Sol. Cells 92 (2008) 686.
[32] F.C. Krebs, H. Spanggaard, Significant improvement of polymer solar cell stability, Chem. Mater. 17 (2005) 5235.
[33] F.C. Krebs, K. Norrman, Analysis of the failure mechanism for a stable organic photovoltaic during 10,000 h of testing, Prog. Photovoltaics: Res. Appl. 15 (2007) 697.
[34] E.A. Katz, S. Gevorgyan, M.S. Orynbayev, F.C. Krebs, Out-door testing and long-term stability of plastic solar cells, Eur. Phys. J. Appl. Phys. 36 (2007) 307.